Effects of Acidification with and without Rennet on a Concentrated Casein System: A Kinetic NMR Probe Diffusion Study

Steven Le Feunteun and François Mariette*

Cemagref, Food Process Engineering Research Unit, CS 64426, 17 avenue de Cucillé, 35044 Rennes Cedex, France

Received October 8, 2007; Revised Manuscript Received December 13, 2007

ABSTRACT: The self-diffusion coefficients of 620 and 96 750 g/mol poly(ethylene glycol) (PEG) were measured by pulsed field gradient (PFG)-NMR throughout the coagulation processes of a concentrated casein suspension induced by acidification alone and with the concomitant action of chymosin. The diffusion of water molecules was also investigated during the acidification process. In all experiments, the diffusion coefficient of the molecule studied was modified nonlinearly, and the precise moments at which its evolution changed corresponded to key stages of both coagulation processes. These variations were not directly related to sol−gel transitions as revealed by rheological measurements but were caused by other types of structural changes in the sample whatever its viscoelastic state (solution or gel). The diffusion of the large PEG was very sensitive to variations in the size of the casein particles and the casein aggregates constituting the network before and after gelation, respectively. In contrast, the diffusion of the small PEG and of water was sensitive to changes in the internal structure of the colloidal matter. The evolution of the sample microstructure could thus be monitored by diffusion measurements throughout the coagulation processes. In comparison, rheometry, stiffness measurements, and scanning electron microscopy revealed these modifications in the gel state only.

Introduction

By studying the diffusion of probe molecules of various sizes, information can be obtained on the microstructure of a sample at different length scales.[1,2] Such experiments have therefore been applied to a great variety of matrices, including polymers and proteins in both liquid and gel states.[3−13] The diffusion of poly(ethylene glycol)s (PEGs) measured by pulsed field gradient (PFG)-NMR is probably the most widely used method to perform these investigations. PFG-NMR is a very powerful and nondestructive technique to determine self-diffusion coefficients,[14,15] and PEG molecules selected as probes offer several advantages. They are water-soluble and available in a wide range of molecular weights with low polydispersity indices, and their NMR signal is a sharp band. Moreover, PEGs present very weak interactions with proteins,[16−20] and there are numerous NMR diffusion sequences which include a solvent suppression scheme.[21−24] With the latter two properties, PEG diffusion determined by PFG-NMR techniques makes possible the observation of obstruction effects in real biological matrices, i.e., without the need to resort to the use of heavy water.

We recently investigated the impact of rennet-induced coagulation of a milk system on the diffusion of different PEGs using PFG-NMR.[25] However, rather than performing one experiment before gelation and one after, self-diffusion measurements were repeated throughout the coagulation process. With this experimental design, we showed that probe diffusion was not directly influenced by the formation of a network but was particularly sensitive to the structural modifications that take place during the aging of the gel. Moreover, depending on the probe size, the evolution of their diffusion coefficient was related to changes in gel porosity and in the internal structure of the casein aggregates forming the network. This illustrates the potential of probe diffusion studies to reveal dynamic information on evolving systems and particularly on dairy matrices.

However, rennet-induced coagulation is not the only process used to produce dairy gels. The formation of a milk gel, i.e., the destabilization of the colloidal system of dispersed casein micelles, can be obtained by the enzymatic action of chymosin (contained in rennet), by slow acidification, or by combinations of both.[26] In milk, the stability of casein micelles is provided by the presence of κ-casein molecules protruding from their surface which prevents their aggregation by steric and electrostatic repulsion.[27,28] In all types of coagulation, casein micelles are first destabilized. The casein particles then aggregate and form a protein network which entraps the serum phase. However, the enzymatic and acid processes are different in many aspects. Whereas chymosin cleaves off the κ-casein molecules, acidification leads to several complex mechanisms before gel formation which have only partially been explained to date. The resulting gel properties are very different according to the process employed, and moreover they depend on various parameters such as temperature, milk pretreatment, and casein concentration.[26,29] The number of influencing parameters rises when combining chymosin action and acidification, particularly because there is considerable synergy between these two processes. A wide variety of coagulation processes and hence products can therefore be achieved, though many mechanisms remain unclear. Probe diffusion studies during such types of transformation may thus provide valuable information on the processes themselves and characterize the impact of various parameters.

The aim of the present study was to investigate the sensitivity of probe diffusion to the structural changes that occur during the coagulation of a casein suspension induced by acidification alone and with the concomitant action of chymosin. The self-diffusion of a small and a large PEG were investigated by PFG-NMR throughout each type of coagulation, and that of water was studied during acid-induced coagulation. For both processes, the sol−gel transition was characterized by rheom-

* Corresponding author: Tel 33 (0)223482121; Fax 33 (0)223482115; e-mail Francois.Mariette@cemagref.fr.

10.1021/ma702248z CCC: $40.75
Published on Web 03/18/2008

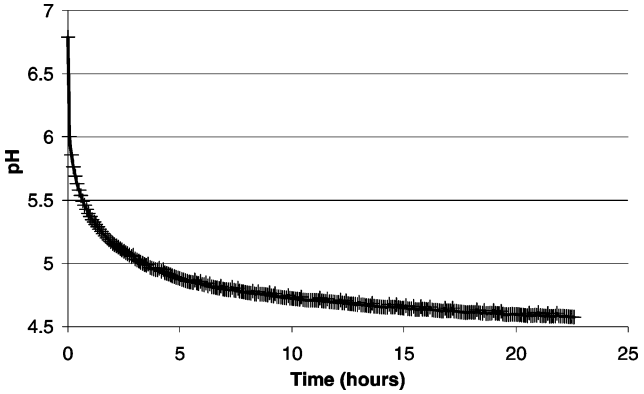

Figure 1. Example of curve representing the recorded values of pH as a function of time after the addition of GDL to a casein suspension maintained at 20 °C. The solid line represents fitting of the data obtained by Table Curve.

etry, and after the onset of gelation, stiffness measurements and scanning electron microscopy (SEM) were used to follow the evolution of the gel properties during aging.

Materials and Methods

Materials. Native phosphocaseinate powder (INRA, Rennes, France) was used (powder composition was described in ref 25). The PEG polymers were obtained from Polymer Laboratories (Marseilles, France), with average molecular masses of 620 and 96 750 g/mol. Both polymers had the same low polydispersity index of 1.06, as indicated by the suppliers. All polymers, sodium azide (NaN_3) (Merck, Darmstadt, Germany), sodium chloride (NaCl), and Glucono-Delta-Lactone (GDL) with a purity above 99% (Sigma-Aldrich, Steinheim, Germany) were used without further purification. The chymosin solution used was Chymax-Plus purchased from Chr-Hansen (Arpajon, France).

Acid and Combined Coagulations. All casein suspensions contained 16.18 ± 0.09 g of casein for 100 g of H_2O and were prepared according to the protocol described in ref 25. To start the acidification process, GDL was added to the casein suspension at the proportion of 4.10 g to 100 g. A chronometer was started at the same time ($t = 0$ s), and the solution was vigorously stirred for 3 min. This procedure provided a pH of around 4.6 at $t = 24$ h. The same procedure was used to form combined gels, except that, in addition to GDL, 700 μL of a chymosin dilution was added for 100 g of casein suspension. The chymosin dilution (1 mL in 99.0 g of distilled water) was always prepared and stored at 4 °C ~20 min before each inoculation. Samples were then rapidly prepared for NMR and dynamic rheological measurements, whereas samples were stored at 20 °C before analysis for SEM and puncture experiments. No shrinkage of the gel was observed during the time scale of the experiments.

pH Measurements. The pH was 6.80 in all the casein suspensions prepared (Schott, pH combination electrode type no. N6280, Germany). In order to follow the acidification kinetics, the pH electrode was placed in an extra amount of sample maintained at 20 °C in a water bath after the total dissolution of the gelling agent-(s). The pH meter was connected to a data logger to record the pH every 5 min (STARLOG, Macro data logger, model 7000B). An example of the curves obtained is presented in Figure 1. The equation relating the time after the addition of gelling agent(s) and pH was obtained by fitting all the data by Table Curve. This procedure enabled us to plot our diffusion and viscoelastic results against pH.

Dynamic Rheological Measurements. The viscoelastic properties of both gels were studied with a controlled stress rheometer (Rheostress RS150, Haake, Germany) using a double-gap cylinder sensor (DG41). The temperature was maintained at 20 °C, and the surface of the sample was covered with silicone oil to prevent evaporation. The storage modulus (G') and the loss modulus (G'') were recorded at a frequency of 1 Hz, and the rheometer was programed to adjust the stress automatically to provide a strain of 0.5%, which was found to be within the linear viscoelastic region of the samples. The phase angle (δ) was calculated according to the equation $\delta = \tan^{-1}(G''/G')$.

Puncture Tests. Penetration measurements were performed with an Instron Universal Testing Machine 5500 (Instron Ltd., France) monitored by the Merlin software. A flat end puncture probe with a diameter of 12.5 mm was pushed into the sample at a speed of 100 mm/min. The depth of penetration into the sample was 8 mm, and the data sampling rate was 50 points/s. The stiffness (slope of the linear part of the curve, representing the elastic deformation, N/mm) and the hardness (strength at the ultimate depth, N) or the strength at fracture (N) when it occurred were calculated.

Scanning Electron Microscopy (SEM). Images were obtained with a scanning electron microscope (Jeol JSM 6301F) operating at an acceleration voltage of 9 kV. The images were produced by CMEBA (France, Rennes). The detailed protocol concerning sample preparation was previously given in ref 25.

Self-Diffusion Measurements. All measurements were conducted at 20 ± 0.1 °C, and the series of diffusion coefficients during the coagulation processes were obtained according to the procedure described in ref 25.

Water self-diffusion was measured on a 20 MHz Bruker spectrometer equipped with a field gradient probe with a spin-echo sequence (PFG-SE). The NMR tubes had an internal diameter of 8 mm, and calibration of the strength of gradients was performed with a sample of pure water of a known self-diffusion coefficient at 20 °C ($D_{H_2O} = 1.98 \times 10^{-9}$ m^2 s^{-1}). Ten values of gradient strength (g) ranging between 0.6 and 3.2 T/m were used during each measurement. Four scans were carried out, and the recycle delay was set at five T_1. The gradient length (δ) and the diffusion interval (Δ) were 0.5 and 5.0 ms, respectively.

PEG self-diffusion measurements were performed on a 500 MHz Bruker spectrometer equipped with a field gradient probe with 5 mm NMR tubes. Diffusion spectra were acquired with a stimulated echo sequence using bipolar gradients (STE-BP) and a 3−9−19 WATERGATE pulse scheme to suppress the water signal. Experiments were carried out with 16 different values of g, ranging from ~0.25 to 5.00 T/m and with $\delta = 1.0$ ms. Sixteen scans were undertaken, and the recycle delay was set at three T_1. Depending on the molecular weight of the PEG studied, Δ was adjusted to obtain a diffusion distance $z \sim 1.5$ μm in the casein suspension, in accordance with the Einstein equation $z = (2D_{PEG}\Delta)^{1/2}$. This procedure enabled molecular probes to cover a much greater distance than the casein micelle diameter (diameter around 150 nm[30]).

NMR Processing Methods. All the data processing was performed with Matlab software. Monte Carlo simulations were used for error calculations with 200 iterations. All self-diffusion coefficients were calculated from the following equation:

$$I/I_0 = \sum_i p_i \exp(-kD_i) \quad (1)$$

where I_0 is the signal intensity in the absence of gradients, D_i the self-diffusion coefficient of the ith component, p_i the fractional proton number of the ith component, and $\sum p_i = 1$ (in this study, i was one or two). The values taken by k in a classic spin-echo sequence (as for water self-diffusion measurements) are given by the following equation:

$$k = \gamma^2 g^2 \delta^2 \Delta \quad (2)$$

However, in a STE−BP NMR sequence with a WATERGATE scheme (as for PEG self-diffusion measurements) the equation is transformed into

$$k = \gamma^2 g^2 \delta^2 (\Delta - \delta/3 - \tau/2) \quad (3)$$

Here, γ is the gyromagnetic ratio (for protons, $\gamma = 26.7520 \times 10^7$ rad T^{-1} s^{-1}), g the amplitude of the gradient, δ gradient duration,

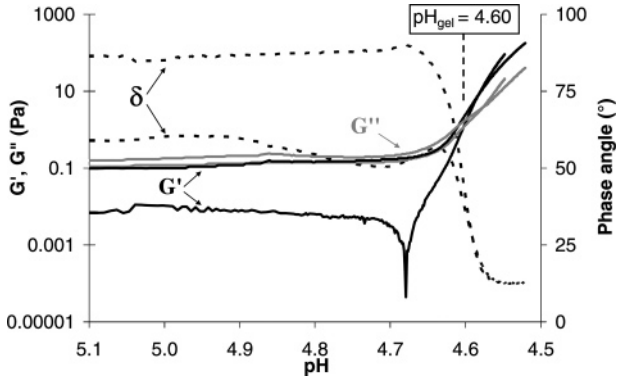

Figure 2. Evolution of storage modulus (G'), loss modulus (G''), and phase angle (δ) as a function of pH during acid coagulation (two repetitions).

Δ the time between the leading edges of gradients, and τ the time between the end of each gradient and the next radio-frequency pulse.

The self-diffusion coefficients of PEGs in the suspensions and all those obtained for water were calculated by fitting eq 1, with $i = 1$, to the raw NMR data. However, the gluconic acid which is progressively formed by hydrolysis of GDL presented an overlapping signal with those of PEGs at a shift of ~3.6 ppm. For the 96 750 g/mol PEG, this polluting signal was totally attenuated in the fourth spectrum of the diffusion spectra. The results for this polymer in the presence of gluconic acid were therefore determined by fitting eq 1, with $i = 1$, after eliminating the first three intensities.

However, the diffusion coefficient of the 620 g/mol PEG was close enough to that of the gluconic acid (180 g/mol) to render the separation of each component by a biexponential fit ineffective, i.e., eq 1 with $i = 2$. To overcome this problem, the diffusion coefficient of the gluconic acid was always determined from an isolated and specific peak of the latter. The proportion of this polluting signal contributing to the NMR band of interest was then estimated. For the first PEG diffusion value measured in the presence of gluconic acid, i.e., at pH ~ 6, the proportion of the gluconic acid signal was obtained by taking an isolated casein signal as reference. For subsequent values, since the sample remained in the tube inside the NMR spectrometer, the increasing proportion of gluconic acid polluting the PEG signal was estimated according to the evolution of the total signal area (PEG + gluconic acid) in the absence of gradients. The diffusion coefficient of gluconic acid and its fractional proton number were finally reintroduced in eq 1 with $i = 2$ to determine the diffusion coefficient of the small polymer.

Normalization of the Self-Diffusion Coefficients. The self-diffusion coefficients obtained in casein suspensions and gels cannot be directly compared because the hindrance caused by the addition of GDL must be considered. This effect was previously investigated in D_2O solutions, and it was shown that the reduction in the probe diffusion rate was proportionally the same whatever the PEG molecular weight.[11] The effect of the addition of GDL was thus explained by an increase in bulk viscosity. In H_2O, this caused exactly the same hindrance as that observed in D_2O (data not shown). For all the molecules studied, the self-diffusion coefficients obtained after the addition of GDL were thus corrected according to the equation previously described in ref 11:

$$D_{\text{corrected}} = D_{\text{measured}} + 0.0235[\text{GDL}]$$

where [GDL] is the mass of GDL added, expresses as a percentage of the total sample mass.

Results

Characterization of Acid-Induced Coagulation. The storage modulus (G'), the loss modulus (G''), and the phase angle (δ) recorded during the acidification of a concentrated casein suspension are given in Figure 2 as a function of pH for two repetitions. Not too much importance should be attached to the differences between the two repetitions before the sol−gel transition (i.e., above pH = 4.65) because the values of G' and G'' measured were still very low (less than 1 Pa) and hence imprecise. The pH at onset of gelation, defined as the pH at which G' and G'' were equal, was pH$_{gel}$ = 4.60, which corresponded to a time after the addition of GDL t_{gel} = 20 h 35. Beyond pH = 4.55, G' and G'' continued to increase while δ stabilized at 13°. Note that a plateau was really observed since the phase angle remained stable for several hours before we stopped the experiment.

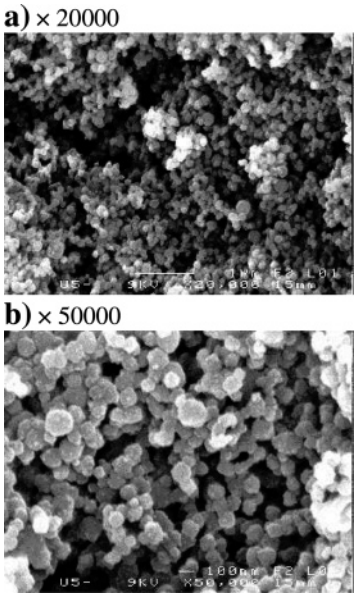

Figure 3. SEM images of an acid gel at $t = 48$ h (pH ~ 4.5) at two magnifications: (a) ×20 000 and (b) ×50 000.

Table 1. Textural Properties of the Acid Gel at Different Times after the Addition of GDL at 20 °C (pH ~ 4.5 at All Times)

time after addition of GDL	stiffness (N/mm)	hardness (N)
41 h 53	0.018	0.17
44 h 41	0.025	0.23
47 h 56	0.032	0.26
49 h 10	0.033	0.26

In the hours after the onset of gelation, the gel was not solid enough to produce SEM images or to conduct stiffness measurements. These experiments were therefore performed only at around $t = 48$ h when the pH of the sample was stabilized just above 4.5. As can be observed in Table 1, the hardness and the stiffness values measured were very low and increased very slowly with time, in accordance with our macroscopic observations. At this moment, the gel structure consisted of an assembly of small and spherical particles (Figure 3). Although these particles were necessarily connected since a gel was formed, no fusion between them was observed.

Self-Diffusion during Acid-Induced Coagulation. Above pH = 4.7, although the rheological properties of the sample remained stable, wide variations in the self-diffusion coefficients of both PEGs and water occurred, as illustrated in Figures 4 and 5, respectively. All curves could be broken down into three different phases. Between the initial pH and pH ~ 5.9, the diffusion coefficients of the PEGs were enhanced, whereas that of water should be considered stable since the apparent increase was not significant. Below pH ~ 5.9, the diffusion rate of all molecules then decreased until pH = 4.9 was reached. They increased to different extents thereafter until the end of the

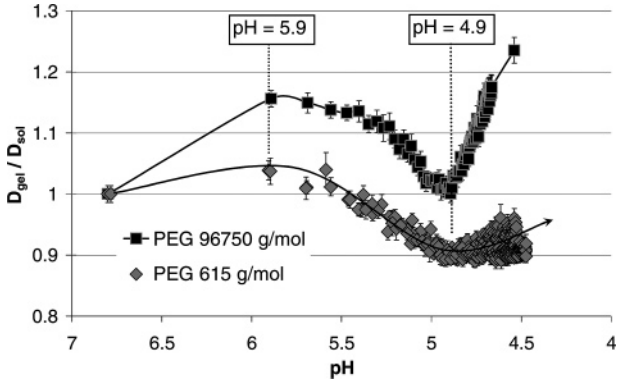

Figure 4. Evolution of a self-diffusion coefficients of 96 750 g/mol PEG and the 620 g/mol PEG (two repetitions) as a function of pH during acid coagulation. Error bars represent the uncertainties given by the Monte Carlo simulations, and solid lines are guides for the eyes.

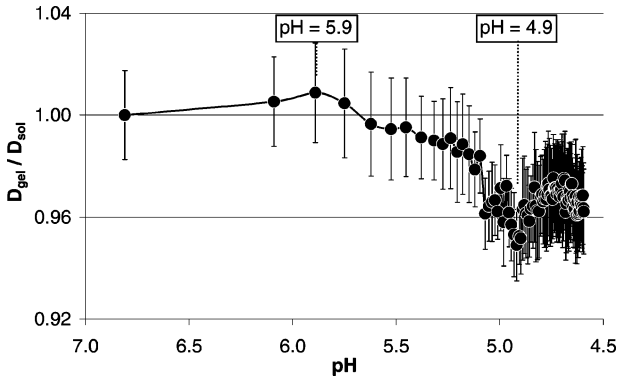

Figure 5. Evolution of self-diffusion coefficient of H_2O as a function of pH during acid coagulation. Error bars represent the uncertainties given by the Monte Carlo simulations, and the solid line is a guide for the eyes.

experiments (at pH ∼ 4.55). Nevertheless, depending on the size of the diffusing molecule, two differences emerged, indicating that scaling effects must be considered. First, in agreement with previous findings,[10,11,25] the extent of the variations was greater for larger probes. Second, the relative size of the decrease, i.e., the second phase, was proportionally larger for smaller molecules. As a result, the diffusion of the largest PEG was increased overall in contrast to that of water and the small PEG. It should also be noted that the diffusion of gluconic acid (180 g/mol) followed the same evolution as that observed for the 620 g/mol PEG (data not shown).

The results obtained for the largest PEG are in line with a previous study in which diffusion measurements were performed before and after acid coagulation in D_2O systems.[11] For water[11,31] and a small probe such as the 620 g/mol PEG,[11] the impact of the acid coagulation was previously considered to be negligible. In fact, our findings confirm that the initial and final values are very close, but they also show that the decrease in pH does have an influence on the diffusion of these molecules. Moreover, the present results demonstrate that the sol−gel transition is not the phenomenon explaining the impact of coagulation on probe diffusion. Other modifications of the matrix, to which rheological measurements were not sensitive, need therefore to be considered.

Characterization of Combined Coagulation. When rennet was added, the onset of gelation (characterized by $pH_{gel} = 5.53$ and $t_{gel} = 50$ min) took place much more rapidly because of the action of chymosin (Figure 6). After the end of the sol−gel transition (from pH ∼ 5.4), while δ was stable around 16°, G' and G'' continued to increase, indicating that the gel became

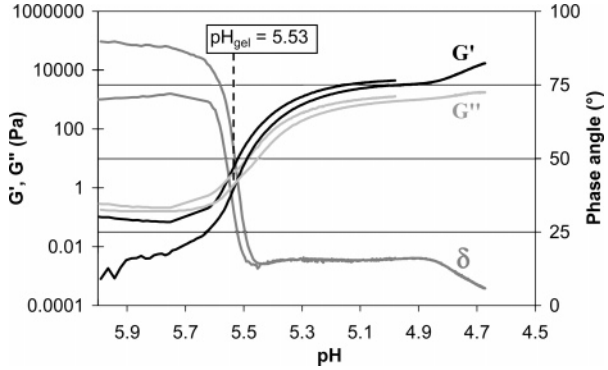

Figure 6. Evolution of storage modulus (G'), loss modulus (G''), and phase angle (δ) as a function of pH during combined coagulation (two repetitions).

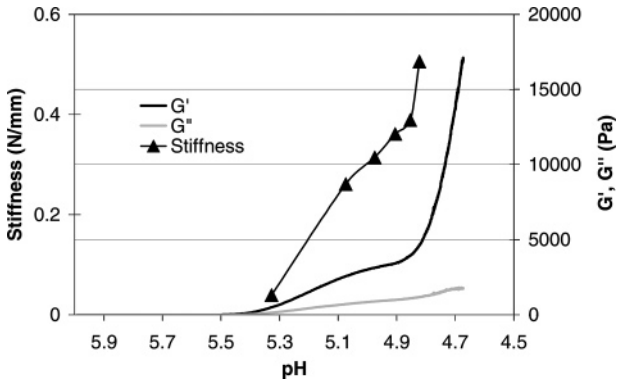

Figure 7. Evolution of storage modulus (G'), loss modulus (G'') and stiffness as a function of pH during combined coagulation.

stiffer. In addition, G'', and to a greater extent G', increased more rapidly, causing a second fall in the phase angle from pH ∼ 4.9 (Figure 6**)** and a more rapid increase in gel stiffness, as shown in Figure 7. All these elements demonstrate that significant changes occurred in the structural organization of the sample after pH = 4.9. The nature and the number and/or strength of the binding forces necessarily changed during this interval. When the experiment was stopped (at $t = 16$ h 25 and pH = 4.67), the phase angle had reached a value of 5.8°, indicating that the gel had become very elastic. Note that all these rheological findings are in very good agreement with previous studies performed on combined gels.[32,33]

SEM images obtained at different times after gel formation are presented in Figure 8. As can be seen from Figure 8a,c,e, the gel microstructure appeared homogeneous at a length scale of a few micrometers at all pH. Figure 8a,b shows a very similar network structure after gel formation (pH = 5.15) to that observed in the acid gel, i.e., small spherical particles and small pores. The matrix organization had greatly changed at pH = 4.78 (Figure 8c,d). The microstructure appeared much more branched, with larger pores. The network consisted of large casein aggregates and thick strands, indicating that the small particles had fused together. After 24 h (pH = 4.56), the same type of organization was observed but with larger empty spaces, indicating that the gel structure had continued to evolve (Figure 8e,f). Images during the hours following network establishment revealed that a new type of organization was being formed, progressively evolving toward a more "open" microstructure.

Self-Diffusion during Combined Coagulation. As shown in Figure 9, until pH = 5.27 was reached, the diffusion of the 96750 g/mol PEG did not depend on the coagulation process since the same behavior was observed when the suspension was acidified without addition of rennet. During this first phase, all

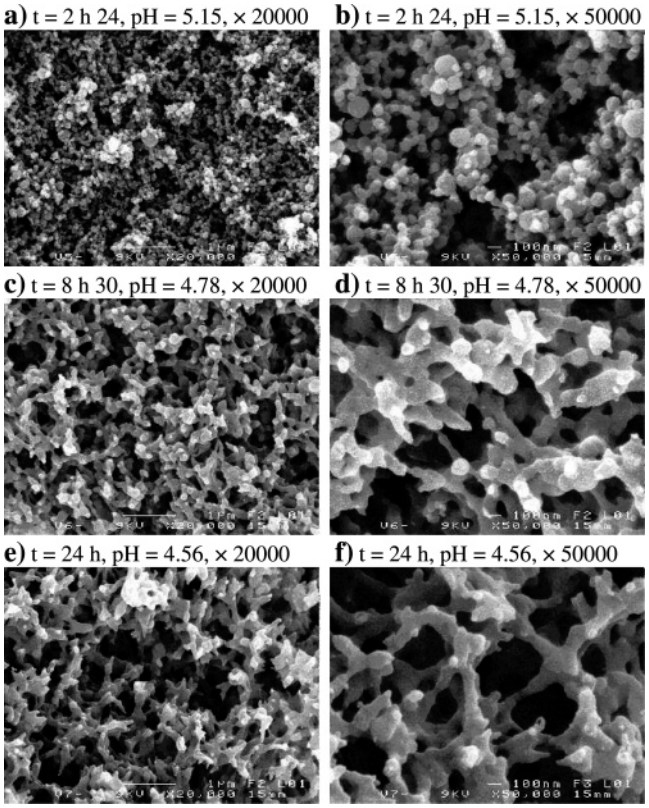

Figure 8. SEM images of combined gels at two magnifications (×20 000 and ×50 000) at different times after the addition of chymosin and GDL: (a, b) $t = 2$ h 24, pH = 5.25; (c, d) $t = 8$ h 30, pH = 4.78; and (e, f) $t = 24$ h, pH = 4.56.

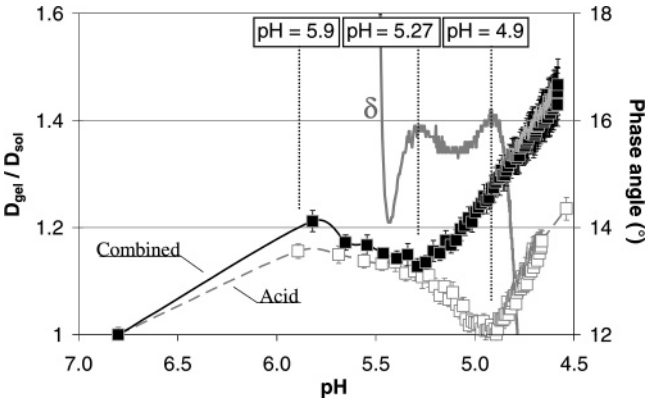

Figure 9. The 96 750 g/mol PEG self-diffusion coefficient as a function of pH with an enlargement of the evolution of the phase angle during combined coagulation. Diffusion of this probe during acid coagulation is also represented for comparison. Error bars represent the uncertainties given bu the Monte Carlos simulations, and the black solid line and the dotted grey line are guides for the eyes.

variations can therefore be explained by pH effects. However, in contrast to what was observed during acidification, a regular and sharp increase in the PEG diffusion rate occurred below pH = 5.27. During this second phase, the self-diffusion coefficient of the 96 750 g/mol PEG was therefore strongly affected by the process used. Moreover, and as already observed during chymosin-induced coagulation,[25] the moment at which the diffusion rate of this probe started to rise was concomitant with a small and local maximum in the phase angle after the end of the sol−gel transition (pH = 5.27). This result therefore confirms previous findings and the sensitivity of the 96 750 g/mol PEG diffusion to phenomena taking place during the gel aging phase. In contrast, the evolution of the 620 g/mol PEG

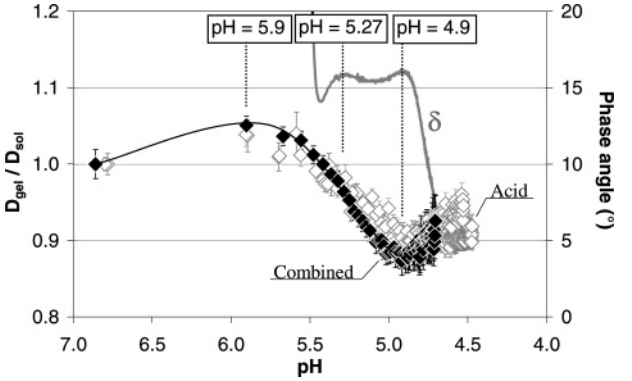

Figure 10. Enlargement of the evolution of the phase angle during combined coagulation and the 620 g/mol PEG self-diffusion coefficient as a function of pH during both acid and combined coagilation processes. The solid black line is a guide for the eyes.

diffusion during the combined coagulation and that obtained during acidification alone were almost identical (Figure 10). Acidification was thus clearly the main factor influencing the diffusion of this small probe while the chymosin action and the aggregation stage had only a minor influence.

Discussion

A casein micelle suspension consists of roughly spherical particles with a mean diameter around 150 nm[30] dispersed in water. The casein micelle structure is still a matter of debate, but recent studies[26,34−36] have shown that caseins are partly linked together by colloidal calcium phosphate nanoclusters, in agreement with the "open structure" models such as those proposed by Holt and Horne[28] and the dual-binding model of Horne.[34] As observed experimentally, these models involve a more or less spherical, highly hydrated, and fairly open particle. In agreement with this description of casein micelles and their reported permeability to large molecules,[37−42] it has been shown that, in contrast to water molecules and a 620 g/mol PEG, a 96 750 g/mol PEG cannot or can hardly diffuse through casein particles.[25] Moreover, the compaction of the casein network which takes place during the gel aging phase of enzymatic-induced coagulation[43,44] was found to cause an increase in the diffusion rate of a 96 750 g/mol PEG but a reduction in that of a 620 g/mol PEG. The diffusion of the large polymer therefore appeared to be mainly sensitive to changes in the gel porosity whereas that of the small probe seemed to be mainly influenced by changes in the internal structure of the network. With these previous findings on probe diffusion in dairy matrices, and existing knowledge concerning coagulation processes, it is possible to propose an explanation for our diffusion results.

1. Self-Diffusion during Acidification. In the case of enzyme-induced coagulation, the diffusion rate of different PEGs did not vary before the network formation was completed.[25] This could be explained simply since no great changes are thought to occur in the sample microstructure before gelation. However, during acidification the diffusion of all the molecules investigated was modified before the sol−gel transition (Figures 4 and 5), and several important physicochemical changes are known to take place in the sample. The overall charge of casein particles, their protein and mineral composition, and their water content, often referred as their hydration, are all modified nonlinearly upon acidification.[45−47] All these phenomena reflect or cause changes in the sample structure and are often broken down into different phases which precisely match with those observed in our diffusion results. Depending on the pH range being considered and the diffusing molecule size, it is thus

possible to relate our diffusion findings to structural modifications occurring at different length scales.

From the initial pH to 5.9, the most remarkable event taking place is a progressive decrease in the casein particle hydration, which reaches a minimum at pH ~ 5.9. At this pH value, about 15%[45−49] of the water contained by the colloidal particles has been released in the aqueous phase, and this causes a reduction in the mean particle size as observed by diffusing wave spectroscopy experiments.[50−52] In fact, as the pH decreases, it progressively approaches the isoelectric pH of caseins (pH_i ~ 4.6[45−49]). This loss of solvent is therefore thought to result from enhanced electrostatic attraction between caseins and in particular from the collapse of the κ-casein layer.[45−52]

Since the 96 750 g/mol PEG could not or could hardly diffuse through casein particles, the reduction in casein particle size can be viewed as a decrease in the volume occupied by obstructing elements. More space was thus accessible to this large polymer, and its diffusion coefficient consequently increased (Figure 4). For the 620 g/mol PEG, the increase was smaller but significant, indicating that its diffusion was also sensitive to the variations in particle hydration. In fact, since this small polymer may diffuse through casein particles, the particle compaction should at least partially balance the effects of the enhanced casein-free volume. This would explain the smaller amplitude of variations observed. When the diffusing molecule size was further decreased, it can be seen that molecular diffusion was progressively less influenced by variations in hydration since that of water was not significantly modified at pH = 5.9 (Figure 5). This is understandable when considering that, in agreement with previous studies,[9,31] water molecules were so small that the obstruction effects they experience were principally caused by the proteins themselves and not or only slightly by the way they hold together.

From pH = 5.9 to 4.9, three main phenomena occur. First of all, solubilization of casein molecules occurs during this phase and reaches a maximum at pH ~ 5.5 at 20 °C.[46,47,53] Although this should at least affect the diffusion of the 96 750 g/mol PEG, since there are fewer soluble proteins at pH ~ 4.9 than at pH = 5.9, such a phenomenon cannot explain the overall decreases observed in this pH range (Figures 4 and 5). Second, particle hydration is known to return progressively to about its initial value. The details of the mechanism explaining this swelling remain unclear, but it is generally attributed to the solubilization of the colloidal calcium phosphate (CCP), which constitutes the third important event occurring in this pH range. In fact, the CCP, which contributes considerably to casein micelle integrity,[46,47,54] is progressively solubilized as soon as acidification is in progress, but process of this dissolution becomes faster below pH ~ 6.0, and at pH = 4.9 all the calcium phosphate has been transferred into the serum phase.[38,46,47,53,55] This necessarily alters the cohesion of the supramolecular edifices, and casein particles therefore undergo structural reorganization which is thought to cause the particle swelling.[47] Besides, although nothing particular was observed by rheometry around pH = 4.9 during acidification (Figure 2), the evolution of the physical properties of the fresh combined gel was clearly modified at pH = 4.9 (Figures 7 and 9). In fact, this only reflects the lower sensitivity of rheological experiments to structural changes occurring in a liquid compared to a gel, especially for such highly concentrated samples.

As during the first phase, the increase in particle hydration seemed to be the key factor explaining the results we obtained with the 96 750 g/mol PEG (Figure 4). The lowest hydration, determined by ultracentrifugation and pellet drying, is reported to occur around pH = 5.2[46,47] rather than at pH = 4.9, but the accuracy of the method employed is debatable, and several parameters may explain this shift. Indeed, the precise pH at which the acidification effects take place depends on numerous factors such as the acidification rate,[49,55,56] the casein concentration,[46,57] and the composition of the aqueous phase.[47,58−60] This shift toward lower pH values was moreover confirmed by the onset of gelation which occurred at pH_{gel} = 4.60 (Figure 2) in our experiments, whereas it is generally reported to take place at around pH = 4.8 in acidified skim milks.[46,53,61]

As observed for the large PEG, the diffusion of water molecules and of the 620 g/mol PEG also decreased until pH = 4.90 was reached (Figures 4 and 5). However, according to the extent of these reductions, they can only be partially attributed to particle swelling since the relative proportions of the three phases no longer correspond to the evolution of particle hydration. The impact of the calcium phosphate itself on the diffusion of water and of the probes may have an influence, but this explanation alone seems to be insufficient to explain such degrees of reduction and their dependence on probe size. However, the structural reorganization of the casein particle can explain these reductions by considering that water molecules, and the 620 g/mol PEG can less easily diffuse through colloidal particles as they became rearranged. Since native casein micelles are thought to have a fairly open structure, it would be not surprising that they evolved toward a less permeable structure upon the loss of CCP. This interpretation of the results obtained with the 620 g/mol PEG is moreover consistent with findings reported by Dalgleish et al.[52] on the basis of ultrasonic spectroscopy experiments.

Below pH = 4.9, the amount of water contained by the casein particles again sharply decreases because of neutralization of the general charge until the isoelectric pH of caseins is reached (pH_i ~ 4.6[45−49,62]). As explained for above pH = 5.9, the reduction in particle hydration caused the diffusion of the molecules investigated to increase to different extents depending on their molecular size (Figures 4 and 5). Gelation of the system took place at pH = 4.6 (Figure 2), but no particular changes could be observed in the diffusion curves. In contrast to what the rheological data suggest (Figure 2), our diffusion results showed that acid coagulation should be viewed as a very progressive process, in accordance with the description of a gradually increasing tendency of particles to interact as the pH is reduced.[52] Although the following findings can be ascribed to certain processing parameters, this description was reinforced by our macroscopic observations, the SEM images (Figure 3), and the very low and slowly evolving stiffness (Table 1), which indicate that the network structure has not been subjected to extensive structural rearrangements.

2. Self-Diffusion during Combined Coagulation and the Implications. The 96 750 g/mol PEG diffusion results obtained during combined coagulation can be easily understood because the effects caused by pH and the chymosin action were clearly separated (Figure 9). In the first part of the curve, i.e., above pH = 5.27, the results were totally explained by pH effects as the same curve was obtained during the acidification process. Then at pH = 5.27, while the gel formation with a strong "rennet character" was over, the PEG self-diffusion rate started to increase at the precise moment at which there was a small and local maximum in the phase angle (Figure 9). Below this pH, the PEG diffusion rate regularly increased until the end of the experiment. As during acid coagulation, this polymer was very sensitive to the progressive increase in the casein-free volume and to the formation of more linear diffusion pathways which

accompanied the structural reorganization of the gel, as can be seen from the SEM images (Figure 8). Without considering pH effects, all these findings are in total agreement with the results previously reported during enzymatic coagulation. Since these new results confirm the effects of chymosin action, which were interpreted in detail in ref 25, it is beyond the scope of this paper to discuss these events further here.

The changes in the evolution of gel stiffness and elasticity from pH = 4.9 (Figures 7 and 9) proved that modifications took place inside the network resulting from the total solubilization of the CCP. This mineral loss might also be related to the extensive fusion of the particles forming the network at this point (Figure 8a−d). However, since the results obtained below pH = 5.27 showed that the 96 750 g/mol PEG diffusion was no longer significantly influenced by pH effects (Figure 9), the overall evolution of the network microstructure in terms of added porosity and tortuosity effects was mainly governed by other types of rearrangement process which are known to occur during the aging phase of a chymosin-induced gel.[44] This highlights the importance of considering and obtaining information on the appropriate length scale of the structural rearrangement processes when trying to relate them to certain properties of dairy products.

The first part of the curve, i.e., above pH = 5.27, is also interesting. We previously showed that transfer of the C-terminal extremities of the κ-caseins from the colloidal to the aqueous phase (due to chymosin action) had no effect on the diffusion of the 96 750 g/mol PEG.[25] In addition, we revealed in this study that the increase in the diffusion of this polymer around pH = 5.9 was caused by reduction in particle size, which is precisely attributed to the collapse of these protruding chains,[46−48,50,51] though some authors remain cautious on this issue.[52] If this was the only explanation, we would have expected to observe an attenuation and progressive disappearance of the increase in the diffusion rate of the polymer as the chymosin action took place. Since the results presented in Figure 9 indicate that the size of the casein particles was only pH-dependent until a gel was totally formed (pH = 5.27, t = 50 min), i.e., when a significant part of the κ-caseins had been hydrolyzed (probably around 40−50%[33]), our results suggest that the reduction in particle size observed at pH ∼ 5.9 would more likely be the result of overall particle shrinkage rather than only a collapse of the κ-casein layer.

For the small PEG (Figure 10), the same curves were obtained during both the acid and the combined coagulation. The diffusion of the 620 g/mol PEG was thus not significantly influenced by the considerable differences in sample properties when acidified with or without the addition of chymosin, i.e., sample state (liquid or gel), number or strength of the attractive forces inside the network (see elasticity and stiffness values), sample microstructure at the scale observed in the SEM images, or even the total colloidal volume (see the diffusion results obtained for the large PEG). Besides, it is of note that these different evolutions in particle hydration during the two processes confirm the minor influence of particle volume on the diffusion of the small PEG.

According to previous results obtained during chymosin-induced coagulation,[25] we would nevertheless have expected to observe a slight but progressive decrease in the diffusion of the 620 g/mol probe concomitantly with the network densification. Although the differences between the two curves are so small compared to experimental uncertainties that no conclusion can be drawn, such a phenomenon would be compatible with the apparently greater extent of the decrease between pH = 5.27 and 4.9 (Figure 10). However, below pH = 4.9, the opposite trend to that described during chymosin coagulation was observed; i.e., while a compaction and a stiffening of the casein network took place during aging, the diffusion of the small PEG slightly increased rather than decreased. This implies that the internal structure of the gel with a strong rennet character was greatly modified upon acidification because of CCP solubilization. In terms of permeability to diffusing molecules, the internal structure of the combined network seemed therefore to be similar to that of the acidified casein particles. This is in line with the results of Tranchant et al.[33] reporting that combined gels which first consist of a gel with a strong rennet character evolved from pH ∼ 5.0 toward a gel with a predominantly acid character.

Conclusions

Throughout both acid and combined coagulation processes, the diffusion of a 96 750 g/mol PEG was very sensitive to variations in the size of the casein particle and in the appearance of the network, whereas those of water and of a 620 g/mol PEG were affected by changes in their internal microstructure. Many of the structural modifications occurring in the sample at different levels could thus be revealed, and interesting conclusions on several key points of the milk coagulation processes could be drawn. In addition, it is of note that the duration of diffusion measurements can be reduced and that the use of lactic bacteria instead of GDL seems to be feasible. Both of these modifications would allow the acquisition of more diffusion data at high pH values.

Our results also proved that probe diffusion and rheological experiments are highly complementary. As for rheometry, NMR experiments can be performed continuously on the same sample. This is a great advantage, especially when studying systems that do not react instantaneously to "disturbances" (e.g., acidification of a milk system[63,64]). In addition, whereas rheology permits characterization of the macroscopic behavior of the sample, the diffusion of probes can be used to provide structural information on smaller scales with equal efficiency in both the liquid and gel states. Finally, it should be noted that, in contrast to most of the techniques commonly employed to characterize modification of a microstructure, probe diffusion is even more sensitive to structural changes when samples are concentrated.

All these features demonstrate that kinetic probe diffusion experiments are very valuable to study the coagulation of milk systems and might also be used to investigate the coagulation of other systems (polyacrylamide,[65−67] alginate,[7,68] etc.) and certain phenomena such as postgelation changes.[69]

Acknowledgment. The authors thank the Regional Council of Brittany and SOREDAB for financial support. We are grateful to Armel Guillermo and Arnaud Bondon for their help with NMR experiments and Joseph Le Lannic for assistance with the SEM experiments. We thank Jean-Michel Soulié, Sandrine Eliot-Godéreaux, Pascale Persenot, and Fabien Guitter from SOREDAB for helpful discussions and assistance with the rheological experiments and Minale Ouethrani for active participation in the rheological and SEM experiments.

References and Notes

(1) Trampel, R.; Schiller, J.; Naji, L.; Stallmach, F.; Kärger, J.; Arnold, K. *Biophys. Chem.* **2002**, *97*, 251−260.

(2) Stilbs, P. Characterization mesoscale structure and phenomena in fluids using NMR. In *Mesoscale Phenomena in Fluid Systems*; American Chemical Society: Washington, DC, 2003; Vol. 861, pp 27−43.

(3) Johansson, L.; Shantze, U.; Lofroth, J. E. *Macromolecules* **1991**, *24*, 6019−6023.
(4) Masaro, L.; Ousalem, M.; Baille, W. E.; Lessard, D.; Zhu, X. X. *Macromolecules* **1999**, *32*, 4375−4382.
(5) Matsukawa, S.; Ando, I. *Macromolecules* **1996**, *29*, 7136−7140.
(6) Nyden, M.; Soderman, O.; Karlstrom, G. *Macromolecules* **1999**, *32*, 127−135.
(7) Baldursdottir, S. G.; Kjoniksen, A.-L.; Nystrom, B. *Eur. Polym. J.* **2006**, *42*, 3050−3058.
(8) Croguennoc, P.; Nicolai, T.; Kuil, M. E.; Hollander, J. G. *J. Phys. Chem. B* **2001**, *105*, 5782−5788.
(9) Colsenet, R.; Cambert, M.; Mariette, F. *J. Agric. Food Chem.* **2005**, *53*, 6784−6790.
(10) Colsenet, R.; Soderman, O.; Mariette, F. *Macromolecules* **2005**, *38*, 9171−9179.
(11) Le Feunteun, S.; Mariette, F. *J. Agric. Food Chem.* **2007**, *55*, 10764−10772.
(12) Newling, B. *J. Phys. Chem. B* **2003**, *107*, 12391−12397.
(13) Weng, L. H.; Liang, S. M.; Zhang, L.; Zhang, X. M.; Xu, J. *Macromolecules* **2005**, *38*, 5236−5242.
(14) Price, W. S. *Concepts Magn. Reson.* **1997**, *9*, 299−336.
(15) Price, W. S. *Concepts Magn. Reson.* **1998**, *10*, 197−237.
(16) Atha, D. H.; Ingham, K. C. *J. Biol. Chem.* **1981**, *256*, 12108−12117.
(17) Bhat, R.; Timasheff, S. N. *Protein Sci.* **1992**, *1*, 1133−1143.
(18) Hancock, T. J.; Hsu, J. T. *Biotechnol. Bioeng.* **1996**, *51*, 410−421.
(19) Hermans, J. *J. Phys. Chem.* **1982**, *77*, 2193−2203.
(20) Knoll, D.; Hermans, J. *J. Biol. Chem.* **1983**, *258*, 5710−5715.
(21) Momot, K. I.; Kuchel, P. W. *Concepts Magn. Reson., Part A* **2006**, *28A*, (4), 249−269.
(22) Dalvit, C.; Ko, S. Y.; Bohlen, J. M. *J. Magn. Reson., Ser. B* **1996**, *110*, (2), 124−131.
(23) Hwang, T. L.; Shaka, A. J. *J. Magn. Reson., Ser. A* **1995**, *112*, 275−279.
(24) Price, W. S.; Elwinger, F.; Vigouroux, C.; Stilbs, P. *Magn. Reson. Chem.* **2002**, *40*, 391−395.
(25) Le Feunteun, S.; Mariette, F. *Macromolecules* **2008**, *41*, 2071−2078.
(26) Lucey, J. A. *J. Dairy Sci.* **2002**, *85*, 281−294.
(27) Walstra, P. *J. Dairy Sci.* **1990**, *73*, 1968−1979.
(28) Holt, C.; Horne, D. S. *Netherlands Milk Dairy J.* **1996**, *50*, 85−111.
(29) Van Vliet, T.; Lakemond, C. M. M.; Visschers, R. W. *Curr. Opin. Colloid Interface Sci.* **2004**, *9*, 298−304.
(30) McMahon, D. J.; Brown, R. J. *J. Dairy Sci.* **1984**, *67*, 499−512.
(31) Mariette, F.; Topgaard, D.; Jönsson, B.; Söderman, O. *J. Agric. Food Chem.* **2002**, *50*, 4295−4302.
(32) Noel, Y.; Lehembre, N.; Dulac, A.; Clavaud, M. C. *Lait* **1989**, *69*, 479−490.
(33) Tranchant, C. C.; Dalgleish, D. G.; Hill, A. R. *Int. Dairy J.* **2001**, *11*, 483−494.
(34) Horne, D. S. *Int. Dairy J.* **1998**, *8*, 171−177.
(35) Marchin, S.; Putaux, J. L.; Pignon, F.; Leonil, J. *J. Chem. Phys.* **2007**, *126*.
(36) Horne, D. S. *Colloids Surf., A* **2003**, *213*, 255−263.
(37) Creamer, K.; Berry, G. P.; Mills, O. E. *New Zealand J. Dairy Sci. Technol.* **1997**, *12*, 58.
(38) Dalgleish, D. G.; Law, J. R. *J. Dairy Res.* **1989**, *56*, 727−735.
(39) De Kruif, C. G.; Tuinier, R.; Holt, C.; Timmins, P. A.; Rollema, H. S. *Langmuir* **2002**, *18*, 4885−4891.
(40) O'Connell, J. E.; De Kruif, C. G. *Colloids Surf., A* **2003**, *216*, 75−81.
(41) Schorsch, C.; Carrie, H.; Clark, A. H.; Norton, I. T. *Int. Dairy J.* **2000**, *10*, 519−528.
(42) Schorsch, C.; Carrie, H.; Norton, I. T. *Int. Dairy J.* **2000**, *10*, 529−539.
(43) Mellema, M.; Heesakkers, J. W. M.; van Opheusden, J. H. J.; van Vliet, T. *Langmuir* **2000**, *16*, 6847−6854.
(44) Mellema, M.; Walstra, P.; Van, Opheusden, J. H. J.; Van Vliet, T. *Adv. Colloid Interface Sci.* **2002**, *98*, 25−50.
(45) Vetier, N.; Banon, S.; Ramet, J. P.; Hardy, J. *Lait* **2000**, *80*, 237−246.
(46) Gastaldi, E.; Lagaude, A.; Marchesseau, S.; De La Funente, B. T. *J. Food Sci.* **1997**, *62*, 671−675.
(47) Famelart, M. H.; Lepesant, F.; Gaucheron, F.; Legraet, Y.; Schuck, P. *Lait* **1996**, *76*, 445−460.
(48) Banon, S.; Hardy, J. *J. Dairy Sci.* **1992**, *75*, 935−941.
(49) Banon, S.; Hardy, J. *J. Dairy Res.* **1991**, *58*, 75−84.
(50) Alexander, M.; Dalgleish, D. G. *Colloids Surf., B* **2004**, *38*, 83−90.
(51) Alexander, M.; Corredig, M.; Dalgleish, D. G. *Food Hydrocolloids* **2006**, *20*, 325−331.
(52) Dalgleish, D.; Alexander, M.; Corredig, M. *Food Hydrocolloids* **2004**, *18*, 747−755.
(53) Gastaldi, E.; Lagaude, A.; De La Funente, B. T. *J. Food Sci.* **1996**, *61*, 59−65.
(54) Van Hooydonk, A. C. M.; Hagedoorn, H. G.; Boerrigter, I. J. *Netherlands Milk Dairy J.* **1986**, *40*, 281−296.
(55) Lee, W. J.; Lucey, J. A. *J. Dairy Sci.* **2004**, *87*, 3153−3164.
(56) Vetier, N.; Desobry-Banon, S.; Eleya, M. M. O.; Hardy, J. *J. Dairy Sci.* **1997**, *80*, 3161−3166.
(57) Ozer, B. H.; Stenning, R.; Grandison, A. S,; Robinson, R. K.; *Int. J. Dairy Technol.* **1999**, *52*, 135−138.
(58) Auty, M. A. E.; O'Kennedy, B. T.; Allan-Wojtas, P. Mulvihill, D. M. *Food Hydrocolloids* **2005**, *19*, 101−109.
(59) Schkoda, P.; Hechler, A.; Kessler, H. G. *Int. Dairy J.* **1999**, *9*, 269−273.
(60) Karlsson, A. O.; Ipsen, R.; Schrader, K.; Ardo, Y. *J. Dairy Sci.* **2005**, *88*, 3784−3797.
(61) Famelart, M. H.; Tomazewski, J.; Plot, M.; Pezennec, S. *Int. Dairy J.* **2004**, *14*, 313−321.
(62) Roefs, S. P. F. M.; Walstra, P.; Dalgleish, D. G.; Horne, D. S. *Netherlands Milk Dairy J.* **1985**, *39*, 119−122.
(63) Mariette, F. Marchal, P. *J. Magn. Reson. Anal.* **1996**, *2*, 290−296.
(64) De Kruif, C. G. *J. Colloid Interface Sci.* **1997**, *185*, 19−25.
(65) Okay, O.; Oppermann, W. *Macromolecules* **2004**, *40*, 3378−3387.
(66) Calvet, D.; Wong, J. Y.; Giasson, S. *Macromolecules* **2004**, *37*, 7762−7771.
(67) Gibbs, S. J.; Johnson, C. S. *Macromolecules* **1991**, *24*, 6110−6113.
(68) Baldursdottir, S. G.; Kjoniksen, A. L. *Eur. J. Pharm. Biopharm.* **2005**, *59*, 501−510.
(69) Pacios, I. E.; Pierola, I. F. *Macromolecules* **2006**, *39*, 4120−4127.

MA702248Z